Available online at www.sciencedirect.com
ScienceDirect
Journal of the European Ceramic Society 27 (2007) 2871–2874
www.elsevier.com/locate/jeurceramsoc

Metal–insulator–metal capacitors using $Ba_2Ti_9O_{20}$ dielectric thin film

Jong-Bong Lim [a], Young Hun Jeong [a], Sahn Nahm [a,*], Jong-Hoo Paik [b], Ho-Jung Sun [c], Hwack-Joo Lee [d]

[a] *Department of Materials Science and Engineering, Korea University, 1-5 Ka, Anam-Dong, Sungbuk-Ku, Seoul 136-701, Republic of Korea*
[b] *Korea Institute of Ceramic Engineering and Technology, 233-5 Gasan-Dong, Guemcheon-Gu, Seoul 153-801, Republic of Korea*
[c] *Department of Materials Science and Engineering, Kunsan National University, San 68, Miryong-dong, Gunsan, Jeonbuk 573-701, Republic of Korea*
[d] *New Materials Evaluation Center, Korea Research Institute of Standard and Science, Deaduk Science Town, Taejeon 305-600, Republic of Korea*

Available online 14 December 2006

Abstract

The dielectric properties of $Ba_2Ti_9O_{20}$ film were investigated to evaluate its potential use in metal–insulator–metal (MIM) capacitors. A homogeneous crystalline $Ba_2Ti_9O_{20}$ phase without any second phase developed for the film grown at 700 °C and rapid thermal annealed at 900 °C for 3 min. The 200 nm-thick $Ba_2Ti_9O_{20}$ film showed a capacitance density of 2.0 fF/μm^2 with a low dissipation factor of 0.016 at 100 kHz. The capacitance density of the film was low, but it could be increased by decreasing the thickness of the film. The leakage current density was approximately 0.094 nA/cm^2 at 1 V. A small linear voltage coefficient of capacitance of −690 ppm/V was obtained, together with a quadratic one of −67.41 ppm/V^2 and a small temperature coefficient of capacitance of −168.87 ppm/°C at 100 kHz. All these results show that the $Ba_2Ti_9O_{20}$ film is a good candidate material for MIM capacitors.

Keywords: Dielectric properties; Electrical properties; $Ba_2Ti_9O_{20}$ thin film; Capacitors

1. Introduction

Recently, many investigations have been conducted into materials with a high dielectric constant (k) with the goal of obtaining a high capacitance density. Metal–insulator–metal (MIM) capacitors commonly use SiO_2 or Si_3N_4 dielectrics because they have good voltage linearity properties and thermal stability. However, their capacitance density is very small, because of their low dielectric constant (k).[1,2] An Al_2O_3 film with a thickness of 12 nm exhibited a high capacitance density of 5.0 fF/μm^2. However, it had a large voltage coefficient of capacitance (VCC).[3] An HfO_2 film with a thickness of 56 nm grown by PLD showed small voltage and temperature coefficients of capacitance, but its capacitance density was relatively low.[4] A MIM capacitor was also produced using a Al_2O_3 and HfO_2 laminate structure, however its capacitance density was relatively low.[5] Pr_2O_3 film was also reported to have a high capacitance density, but to exhibit a large VCC.[6] A high capacitance density of 17.0 fF/μm^2 and a low leakage current of 10^{-7} A/cm^2 were obtained from a MIM capacitor made using a ZrO_2 film with a thickness of 12 nm, but the variation of the capacitance with the bias voltage and temperature was not reported.[7]

It is generally recognized that microwave dielectric materials have a high k, high quality factor (Q-factor) and good temperature stability.[8] In particular, $BaTi_4O_9$ ceramics are known to have excellent microwave dielectric properties.[9–11] Moreover, $BaTi_4O_9$ films have been found to exhibit excellent dielectric properties for MIM capacitors.[12,13] The $Ba_2Ti_9O_{20}$ microwave dielectric ceramics was reported by Jonker and Kwestroo and they were found to exhibit good microwave dielectric properties with a high k of 39.8, a high Q-factor of 8000 at 4 GHz and good thermal stability.[14,15] Many investigations have been conducted into $Ba_2Ti_9O_{20}$ ceramics, however, no attempts have been made to use $Ba_2Ti_9O_{20}$ film for MIM capacitors. Therefore, in this work, $Ba_2Ti_9O_{20}$ thin films were formed for the first time and their structural and dielectric properties were investigated, in order to assess their potential use as new dielectric materials for MIM capacitors.

2. Experimental details

The $Ba_2Ti_9O_{20}$ film was grown on Pt/Ti/SiO_2/Si(1 0 0) substrate by RF-magnetron sputtering using a 7.6×10^{-2} m-diameter $Ba_2Ti_9O_{20}$ target which was synthesized by the

* Corresponding author. Tel.: +82 2 3290 3279; fax: +82 2 928 3584.
E-mail address: snahm@korea.ac.kr (S. Nahm).

0955-2219/$ – see front matter © 2006 Elsevier Ltd. All rights reserved.
doi:10.1016/j.jeurceramsoc.2006.11.042

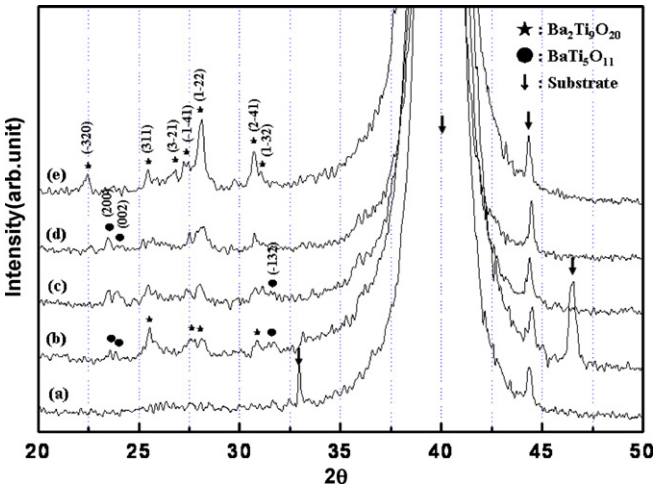

Fig. 1. XRD pattern of the $Ba_2Ti_9O_{20}$ films grown at (a) 700 °C without annealing and grown at (b) room temperature, (c) 300 °C, (d) 500 °C and (e) 700 °C and subsequently annealed at 900 °C for 3 min.

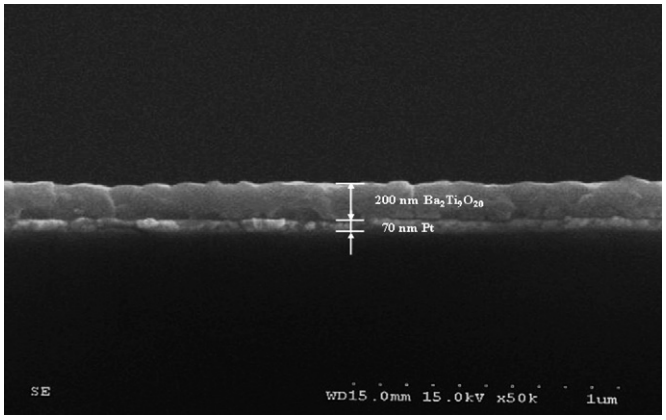

Fig. 2. SEM image of the $Ba_2Ti_9O_{20}$ film grown at 700 °C and annealed at 900 °C for 3 min.

conventional solid state method. Deposition was carried out between room temperature and 700 °C in a mixed oxygen and argon (O_2:Ar = 1:4) atmosphere with a total pressure of 1.13 Pa and a sputtering power of 140 W. Following its deposition, the thin film was subsequently annealed at various temperatures in an O_2 atmosphere using a rapid thermal annealing (RTA) system. The structure of the film was studied using X-ray diffraction (XRD: Rigaku D/max-RC, Japan) and scanning electron microscopy (SEM:Hitachi S-4300, Japan). For the measurement of the dielectric properties, Pt was deposited on the thin film using conventional DC sputtering to form the top electrode of a MIM capacitor. The top electrode was patterned using a shadow mask to form a disk with a diameter of 360 μm. The capacitance and dissipation factor were measured by a precision LCR meter (Agilent 4285A, USA). The leakage current was measured using a source meter (Keithley2400, USA).

3. Results and discussion

Fig. 1(a) shows the XRD pattern of the $Ba_2Ti_9O_{20}$ film grown at 700 °C. No peaks were observed from the crystalline phase of the film. Therefore, it is considered that this film has an amorphous phase. However, it is also possible that the crystalline phase was formed in these films, but that its amount was too small to be detected in the XRD patterns. Fig. 1(b–e) shows the XRD patterns of the films grown at various temperatures and subjected to RTA at 900 °C for 3 min. Peaks for the crystalline $Ba_2Ti_9O_{20}$ phase were found in the all the films. However, for the films grown at temperatures below 700 °C, peaks for $BaTi_5O_{11}$ second phase were also observed. The $BaTi_5O_{11}$ phase was first observed by Tillmanns from the quenched melt of $BaTi_4O_9$, and it has subsequently also been produced by the sol–gel or liquid mixture methods.[16–18] It was also suggested that the $BaTi_5O_{11}$ phase could easily be produced from the amorphous phase. Moreover, $BaTi_5O_{11}$ phase was formed in $BaTi_4O_9$ film when the amorphous $BaTi_4O_9$ film was annealed at low temperature.[19] Therefore, it can be considered that for the $Ba_2Ti_9O_{20}$ films deposited at temperatures below 700 °C, an amorphous phase was formed during the deposition and this amorphous phase was transformed into the crystalline $Ba_2Ti_9O_{20}$ phase and $BaTi_5O_{11}$ second phase during the annealing at 900 °C. However, for the film grown at 700 °C and annealed at 900 °C, it is considered that a small amount of $Ba_2Ti_9O_{20}$ crystals were already formed during its deposition and grew and developed to produce a homogeneous $Ba_2Ti_9O_{20}$ crystalline film without any $BaTi_5O_{11}$ second phase.

The SEM image of the $Ba_2Ti_9O_{20}$ film grown at 700 °C and annealed at 900 °C is shown in Fig. 2. The thickness of the film was approximately 200 nm and a sharp interface was formed between the Pt-bottom electrode and the $Ba_2Ti_9O_{20}$ film.

Fig. 3 shows the capacitance density and dissipation factor of the 200 nm-thick $Ba_2Ti_9O_{20}$ film grown at 700 °C and annealed at 900 °C measured at various frequencies. The capacitance density of this film was 2.0 fF/μm^2 and its frequency dependence was not significant. The effective k value of this film was approximately 44.3, which is similar to that of $Ba_2Ti_9O_{20}$ ceramics. According to the International Technology Roadmap for Semiconductors (ITRS), a capacitance densities of 4.0 fF/μm^2 will be required for the analog capacitor, to be used in the years 2007–2009.[20] The capacitance density of the 200 nm-thick

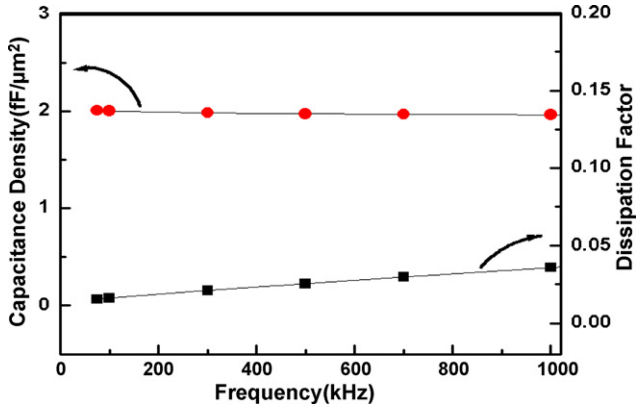

Fig. 3. Capacitance density and dissipation factor of the 200 nm-thick $Ba_2Ti_9O_{20}$ film grown at 700 °C and annealed at 900 °C measured at various frequencies.

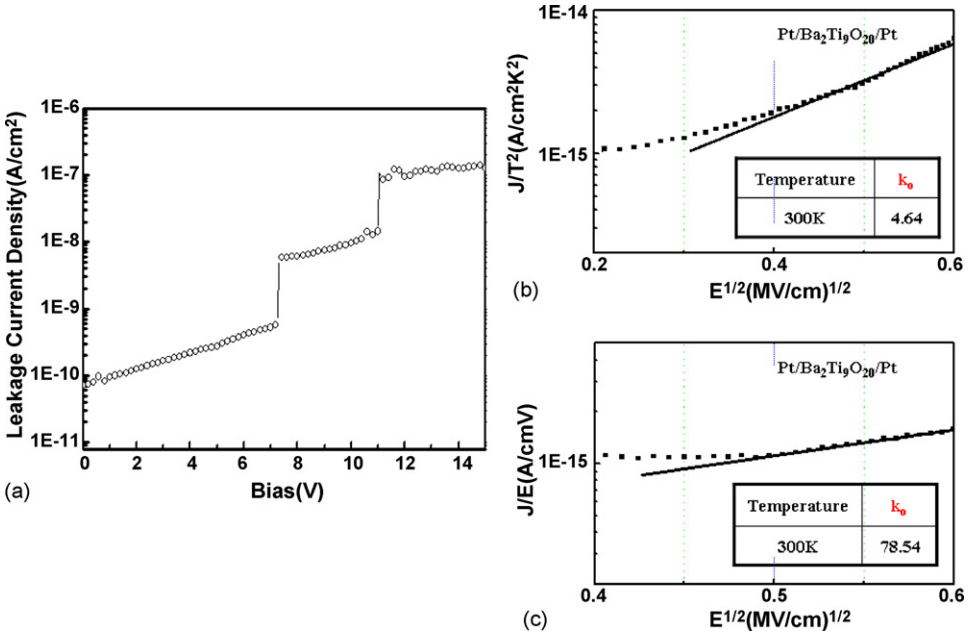

Fig. 4. (a) Leakage current density measured at various applied voltage and the plots of (b) $\log(J/T^2)$ vs. $E^{1/2}$ and (c) $\log(J/E)$ vs. $E^{1/2}$ for the $Ba_2Ti_9O_{20}$ film.

$Ba_2Ti_9O_{20}$ film is too low for it to be used as a MIM capacitor. However, since the thickness of the film is 200 nm, its capacitance density could be increased by decreasing the thickness of the film. The dissipation factor of the $Ba_2Ti_9O_{20}$ film, which is also shown in Fig. 3, was 0.016 at 100 kHz.

The variation of the leakage current density with the applied voltage is illustrated in Fig. 4(a). Leakage current density of this film was low, 0.094 nA/cm^2 at 1 V. More than 90% of the capacitors were not short-circuited till 15 V. According to the ITRS, a leakage current density of 7.0 fA/pF V or lower is required for precision analog capacitors. The leakage current density of the $Ba_2Ti_9O_{20}$ film was approximately 0.47 fA/pF V and therefore satisfied the ITRS requirement. The leakage current mechanism of the $Ba_2Ti_9O_{20}$ film was also studied. There are two leakage current mechanisms for dielectric thin film in a high field: Schottky emission and Poole-Frenkel emission. For Schottky emission, the plot of $\log(J/T^2)$ versus $E^{1/2}$ produces a straight line, where J is a current density, T the temperature and E is the electric field. From the slope of this line we can calculate a dielectric constant in the optical range of frequencies (k_o).[21] If this calculated k_o satisfies the equation $k_o = n^2$, where n is the refractive index of the material,[21] the leakage current mechanism is a Schottky emission.[21,22] On the other hand, a plot of $\log(J/E)$ versus $E^{1/2}$ produces a straight line for the Poole-Frenkel emission and we can calculate k_o from the slope of this line.[21] If this k_o satisfies the equation $k_o = n^2$, where n is the refractive index of the material,[21] the leakage current mechanism is a Poole-Frenkel emission.[21,22] Fig. 4(b and c) shows the plots of $\log(J/T^2)$ versus $E^{1/2}$ and $\log(J/E)$ versus $E^{1/2}$ for the $Ba_2Ti_9O_{20}$ film, respectively. The calculated k_o value obtained from the plot of Fig. 4(b) is 4.64 whereas that obtained from the plot in Fig. 4(c) is about 78.54. On the other hand, the refractive index of most of the ceramics is in the range of 2–3.[23] Therefore, even though we could not obtain the experimental k_o of the $Ba_2Ti_9O_{20}$ film, because its refractive index has not been reported in the literature, the refractive index of the $Ba_2Ti_9O_{20}$ film is considered to be approximately 2–3 and, thus, in all likelihood its k_o value is in the range of 4–9, indicating that its leakage current mechanism is probably Schottky emission.

The linearity of the variation in capacitance with applied voltage or temperature is very important parameters for MIM capacitor. The VCC of the $Ba_2Ti_9O_{20}$ film can be obtained from the capacitance and voltage measurements using the second order polynomial equation, $C(V)/C_0 = \alpha V^2 + \beta V + 1$, where C_0 is the zero-biased capacitance, and α and β represent the quadratic and linear VCCs, respectively.[4] Fig. 5 shows the variation in the capacitance density with the applied voltage at various frequencies for the $Ba_2Ti_9O_{20}$ film grown at 700 °C and subjected to RTA at 900 °C. The VCC increased with increasing frequency

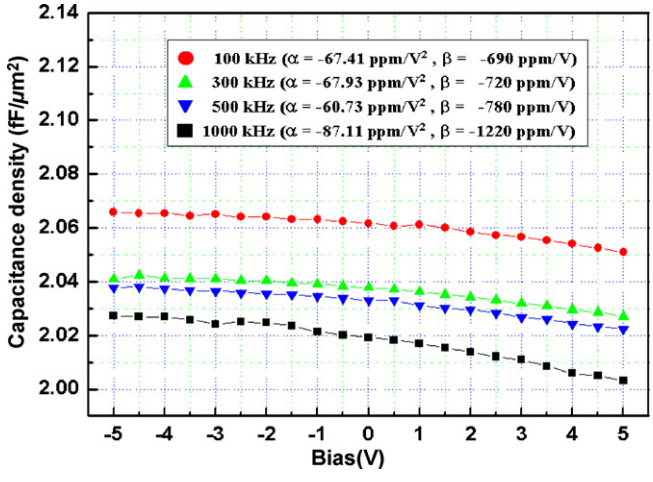

Fig. 5. Variation of the capacitance density of the $Ba_2Ti_9O_{20}$ MIM capacitor measured at various frequencies as a function of the applied voltage.

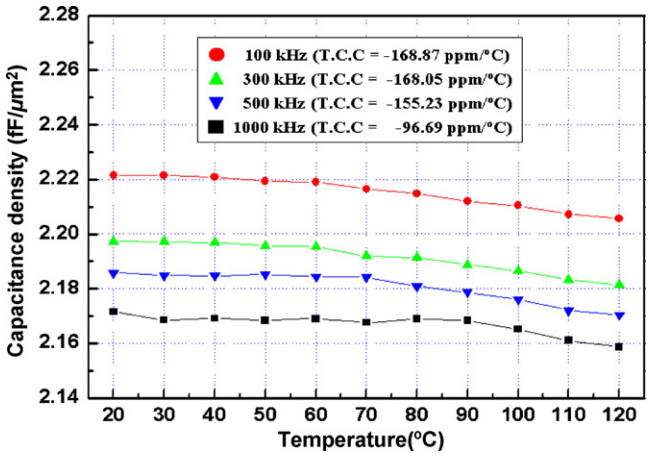

Fig. 6. Variation of the capacitance density of the $Ba_2Ti_9O_{20}$ MIM capacitor measured at various frequencies as a function of the temperature.

but this variation was not significant. For the $Ba_2Ti_9O_{20}$ film measured at 100 kHz, the values of α and β were -67.41 ppm/V^2 and -690 ppm/V, respectively. The quadratic and linear VCCs satisfy the requirement ($\alpha < 100$ ppm/V^2, $\beta < 1000$ ppm/V) for precision analog capacitors. The TCC was also measured from 20 to 120 °C at various frequencies, as shown in Fig. 6. After heating it up to 120 °C, the capacitance of the MIM capacitor was measured at various frequencies during its subsequent cooling. As the temperature increased, the capacitance density decreased, indicating that the $Ba_2Ti_9O_{20}$ film has a negative TCC. The TCC of the $Ba_2Ti_9O_{20}$ film measured at 100 kHz was -168.87 ppm/°C. Therefore, $Ba_2Ti_9O_{20}$ film has very good temperature stability.

4. Conclusions

The homogeneous crystalline $Ba_2Ti_9O_{20}$ phase was well developed for the film grown at 700 °C and rapid thermal annealed at 900 °C for 3 min. The 200 nm-thick $Ba_2Ti_9O_{20}$ film shows a capacitance density of 2.0 fF/μm^2 with a low dissipation factor of 0.016 at 100 kHz. The effective k value of this film is 44.3 which is similar to that of $Ba_2Ti_9O_{20}$ ceramics. The capacitance density of this film is relatively low, but it could be increased by decreasing thickness of the film. The leakage current density of the film was approximately 0.094 nA/cm^2 at 1 V and leakage current mechanism is considered to be Schottky emission. A small linear VCC of -690 ppm/V was obtained, together with a quadratic one of -67.41 ppm/V^2 and a small TCC of -168.87 ppm/°C at 100 kHz. Therefore, the $Ba_2Ti_9O_{20}$ film is a good candidate materials for MIM capacitor. However, since the process temperature used to grow the $Ba_2Ti_9O_{20}$ film is too high for back-end line integration, more research is required to decrease the process temperature without deteriorating the dielectric properties of the film.

Acknowledgements

This work was supported by the Ministry of Commerce, Industry and Energy through the Standardization project and one of the authors also acknowledges that this work was financially supported by the Ministry of Science and Technology through the NRL project.

References

1. Babcock, J. A., Blaster, S. G., Pinto, A., Dirnecker, C., Steinmann, P., Jumpertz, R. *et al.*, Analog characteristics of metal-insulator-metal capacitors using PECVD nitride dielectrics. *IEEE Electron Device Lett.*, 2001, **22**, 230–232.
2. Farcy, A., Torres, J., Arnal, V., Fayolle, M., Feldis, H., Jourdan, F. *et al.*, A new damascene architecture for high-performance metal–insulator–metal capacitors integration. *Microelectron. Eng.*, 2003, **70**, 368–372.
3. Chen, S. B., Lai, C. H., Chin, A., Hsieh, J. C. and Liu, J., High-density MIM capacitors using Al_2O_3 and $AlTiO_x$ dielectrics. *IEEE Electron Device Lett.*, 2002, **23**, 185–187.
4. Hu, H., Zhu, C., Lu, Y. F., Li, M. F., Cho, B. J. and Choi, W. K., A high performance MIM capacitor using HfO_2 dielectrics. *IEEE Electron Device Lett.*, 2002, **23**, 514–516.
5. Ding, S. J., Hu, H., Zhu, C., Li, M. F., Kim, S. J., Cho, B. J. *et al.*, Evidence and understanding of ALD HfO_2/Al_2O_3 laminate MIM capacitors outperforming sandwich counterparts. *IEEE Electron Device Lett.*, 2004, **25**, 681–683.
6. Wenger, C., Darbrowski, J., Zaumseil, P., Sorge, R., Formanek, P., Lippert, G. *et al.*, First investigation of metal-insulator-metal (MIM) capacitor using Pr_2O_3 dielectrics. *Mater. Sci. Semicon. Proc.*, 2004, **7**, 227–230.
7. Lee, S. Y., Kim, H. S., Mclntyre, P. C., Saraswat, K. C. and Byun, J. S., Atomic layer deposition of ZrO_2 on W for metal–insulator–metal capacitor application. *Appl. Phys. Lett.*, 2003, **82**, 2874–2876.
8. Wakino, K., Minai, K. and Tamura, H., Microwave characteristics of (Zn,Sn)TiO_4 and BaO-PbO-Nd_2O_3-TiO_2 dielectric resonators. *J. Am. Ceram. Soc.*, 1974, **67**, 278–281.
9. Negas, T., Yeager, G., Bell, S., Coats, N. and Minis, I., $BaTi_4O_9/Ba_2Ti_9O_{20}$ based ceramics resurrected for modern microwave applications. *J. Am. Ceram. Soc. Bull.*, 1993, **72**, 80–89.
10. Choy, J. H., Han, Y. S., Sohn, J. H. and Itoh, M., Microwave dielectric characteristics of BaO–TiO_2 oxides prepared by citrates route. *J. Am. Ceram. Soc.*, 1995, **78**, 1169–1172.
11. Cernea, M., Chirtop, E., Neacsu, D., Pasuk, I. and Iordanescu, S., Preparation of $BaTi_4O_9$ from oxalates. *J. Am. Ceram. Soc.*, 2002, **85**, 499–503.
12. Jang, B. Y., Kim, B. J., Lee, S. J., Lee, K. J., Nahm, S., Sun, H. J. *et al.*, $BaTi_4O_9$ thin films for high-performance metal-insulator-metal capacitors. *Appl. Phys. Lett.*, 2005, **87**, 112902-1–112902-3.
13. Jeong, Y. H., Lim, J. B., Nahm, S., Sun, H. J. and Lee, H. J., High-Performance Metal-Insulator-Metal Capacitors Using Amorphous $BaTi_4O_9$ Thin Film, *J. Electrochem. Soc.*, in press.
14. Jonker, G. H. and Kwestroo, W., The ternary systems BaO–TiO_2–SnO_2 and BaO–TiO_2–ZrO_2. *J. Am. Ceram. Soc.*, 1958, **41**, 390–394.
15. O'Bryan, H. M., Thomson, J. and Plourde, J. K., A new BaO–TiO_2 compound with temperature-stable high permittivity and low microwave loss. *J. Am. Ceram. Soc.*, 1974, **57**, 450–453.
16. Tillmann, E., Die Kristallstruktur Von $BaTi_5O_{11}$. *Acta Cryst. Sect. B*, 1969, **25**, 1444–1452.
17. Ritter, J. J., Roth, R. S. and Blendell, J. E., Alkoxide precursor synthesis and characterization of phase in the barium-titanium oxide system. *J. Am. Ceram. Soc.*, 1986, **69**, 155–162.
18. Javadpour, J. and Eror, N., Raman spectroscopy of higher titanate phase in the $BaTiO_3$–TiO_2 system. *J. Am. Ceram. Soc.*, 1988, **71**, 206–213.
19. Jang, B. Y., Jeong, Y. H., Lee, S. J., Lee, K. J., Nahm, S., Sun, H. J. *et al.*, Structural variation of the $BaTi_4O_9$ thin films grown by RF magnetron sputtering. *J. Am. Ceram. Soc.*, 2005, **88**, 1209–1212.
20. The International Technology Roadmap for Semiconductors, 2004.
21. Simmons, J. G. 1., In *Handbook of Thin Film Technology*, ed. L. I. Maissel and R. Glang. Mcgraw-Hill Inc., New York, 1970, pp. 14-1–14-32.
22. Sze, S. M., *Physics of Semiconductor*. John Wiley & Sons Inc., New York, 1981, pp. 402–407.
23. Kingery, W. D., Bowen, H. K. and Ujlmann, D. R., *Introduction to Ceramics*. John Wiley & Sons Inc., New York, 1976, pp. 658–676.